MHD simulations of turbulent galactic outflows

Jens Kleimann Horst Fichtner

Theoretische Physik IV
Ruhr-Universität Bochum
Germany

CRC 1491 General Assembly ⋄ 07 November 2023

Project **A4** within CRC 1491

"Magnetohydrodynamical halos of starforming galaxies"

1. Observations: R.-J. Dettmar, M. Stein → (talk by MS)
2. Theory / numerics: H. Fichtner, JK → this talk)

- **Goal**: study turbulence properties of galactic outflows.

Project **A4** within CRC 1491

"Magnetohydrodynamical halos of starforming galaxies"

1. Observations: R.-J. Dettmar, M. Stein → (talk by MS)
2. Theory / numerics: H. Fichtner, JK → this talk)

- **Goal**: study turbulence properties of galactic outflows.
- **Method**: MHD + "fluid-like" equations for turbulence

  $Z^2 = \langle \delta u^2 + \delta b^2 / n \rangle$, $\sigma_c = 2\langle \delta\vec{u} \cdot \delta\vec{b}/\sqrt{n}\rangle / Z^2$, λ_{corr}

  from Reynolds averaging: $\vec{B} = \langle \vec{B} \rangle + \delta\vec{b}$, $\vec{u} = \langle \vec{u} \rangle + \delta\vec{u}$
- Significant synergy effects from recently completed similar work on (inner) heliosheath (with S. Oughton, U Waikato).

Starting from what we know...

Adopted strategy

Start from (working) solar wind setting, then gradually move towards galactic winds, changing one thing at a time:

1. spherical to cylindrical coordinates (same physics)
2. wind source: sphere $\to$ disk(-like surface)
3. first HD, then MHD, then MHD + turbulence

Starting from what we know...

Adopted strategy

Start from (working) solar wind setting, then gradually move towards galactic winds, changing one thing at a time:

1. spherical to cylindrical coordinates (same physics)
2. wind source: sphere $\rightarrow$ disk(-like surface)
3. first HD, then MHD, then MHD + turbulence

- "disk" surface: prolate ellipsoid with semi-axes $\rho_{\rm core}$, $z_{\rm core}$
- initial conditions and $\Phi_{\rm grav}(\vec{r})$ given in terms of

$$R_{\rm e}(\rho, z) := \sqrt{(\rho/\rho_{\rm core})^2 + (z/z_{\rm core})^2}$$

$\Rightarrow$ inner "disk" boundary at $R_{\rm e} = 1$
recovering spherical case if $\rho_{\rm core} = z_{\rm core}$

HD sample run (adiabatic, $T_0 = 0.5\,\mathrm{MK}$, $n_0 = 1\,\mathrm{cm}^{-3}$)

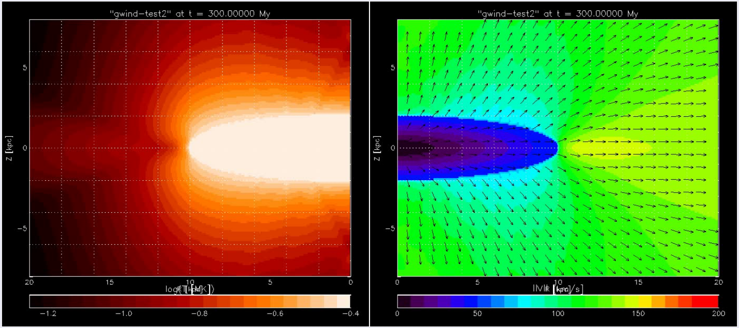

temperature $\log(T)$ velocity $\|\vec{u}\|$

Global parameters:

$\rho_{\text{core}} = 10\,\text{kpc}$, $z_{\text{core}} = 2\,\text{kpc}$, $\gamma = 5/3$, $\mu = 0.62$

MHD sample run ($\vec{B}|_{t=0} = 0.1\,\mathrm{nT}\ \vec{e}_z$)

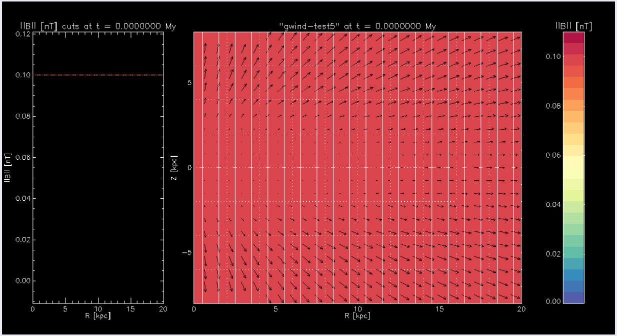

field strength $\|\vec{B}\|$ + field lines (white)

- keep $\vec{u} = \vec{0}$ inside ellipsoid to maintain $\nabla \cdot \vec{B} = 0$

MHD sample run ($\vec{B}|_{t=0} = 0.1\,\mathrm{nT}\ \vec{e}_z$)

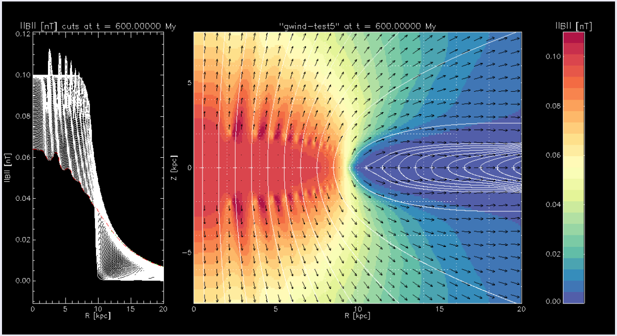

field strength $\|\vec{B}\|$ + field lines (white)

- keep $\vec{u} = \vec{0}$ inside ellipsoid to maintain $\nabla \cdot \vec{B} = 0$
- "ripple" artifacts caused by finite cell size (~ 0.1 kpc); can be eliminated by smoothing the boundary.

Reference benchmark: *"Dynamical Behavior of Gaseous Halo in a Disk Galaxy"* [Habe & Ikeuchi 1980]

- uses standard hydro(!) equations in 2D plus "cooling" term

$$\partial_t e = \ldots - (n\,m)^2 \Lambda(T)$$

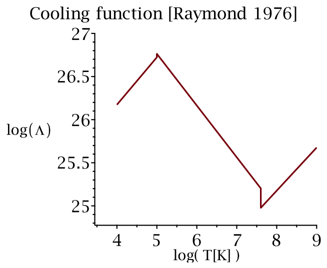

Reference benchmark: *"Dynamical Behavior of Gaseous Halo in a Disk Galaxy"* [Habe & Ikeuchi 1980]

- uses standard hydro(!) equations in 2D plus "cooling" term

$$\partial_t e = \ldots - (n\,m)^2 \Lambda(T)$$

- disk gravity from

$$\Phi_\mathrm{d} = -\sum_{i=1}^{2} \frac{G\,M_i}{\sqrt{\rho^2 + \left(a_i + \sqrt{z^2 + b_i^2}\right)^2}}$$

[Miamoto & Nagai 1975]

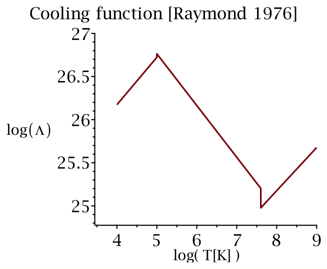

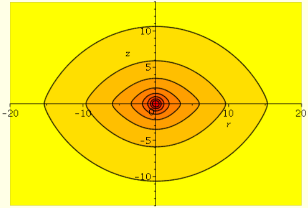

Reference benchmark: *“Dynamical Behavior of Gaseous Halo in a Disk Galaxy”* [Habe & Ikeuchi 1980]

- uses standard hydro(!) equations in 2D plus “cooling” term

$$\partial_t e = \ldots - (n\,m)^2 \Lambda(T)$$

- disk gravity from

$$\Phi_\mathrm{d} = -\sum_{i=1}^{2} \frac{G\,M_i}{\sqrt{\rho^2 + \left(a_i + \sqrt{z^2 + b_i^2}\right)^2}}$$

[Miamoto & Nagai 1975]

- spherical halo potential [Innanen 1973]:

$$\Phi_\mathrm{h} \propto \ln(1 + r/r_0) + (1 + r/r_0)^{-1}$$

- boundary cond.s at $z = 0$, $\rho \in [4, 12]$: T and n fixed, $u_\varphi = \sqrt{(\partial_\rho \Phi_\mathrm{tot})\,\rho}$

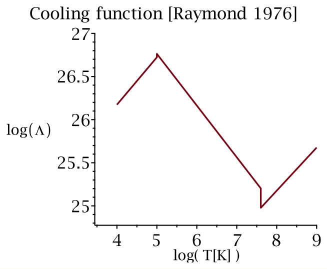

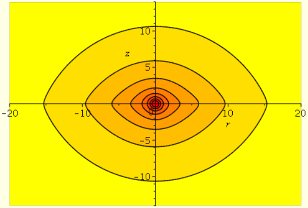

Target work

H&I '80 "wind-type" model ($T_\mathrm{d} = 5\,\mathrm{MK}$, $n_\mathrm{d} = 10^{-3}\,\mathrm{cm}^{-3}$, $\Phi_\mathrm{h} \neq 0$). Right plot: density and temperature at $t = 200\,\mathrm{My}$.

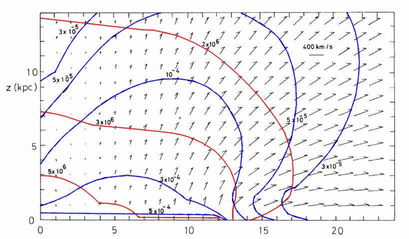

Data from Cronos validation run ($\rho \in [4, 10]$ boundary)

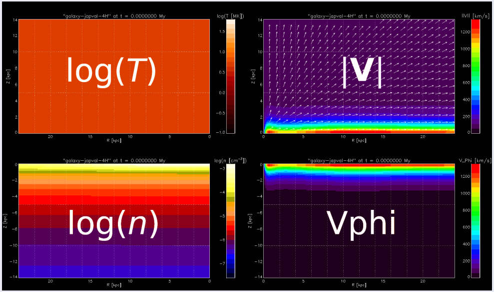

Target work

H&I ’80 “wind-type” model ($T_\mathrm{d} = 5\,\mathrm{MK}$, $n_\mathrm{d} = 10^{-3}\,\mathrm{cm}^{-3}$, $\Phi_\mathrm{h} \neq 0$). Right plot: density and temperature at $t = 200\,\mathrm{My}$.

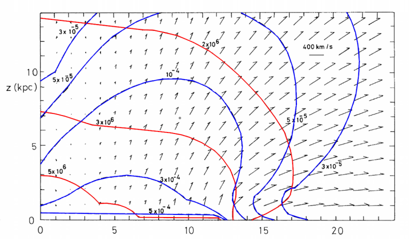

Data from Cronos validation run ($\rho \in [4, 10]$ boundary)

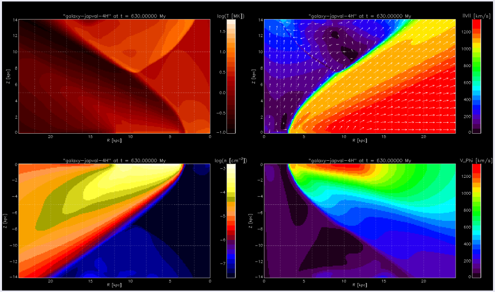

Note that $|u_\varphi|$ is too large (∼5x)

Determining the cause of the near-axis inflow instability

- Closing the "hole" in the disk makes no (big) difference.

Data from Cronos validation run ($\rho \in [0, 10]$ boundary)

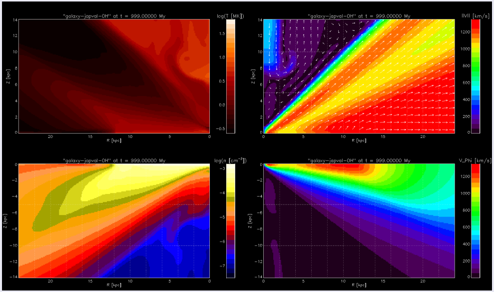

Determining the cause of the near-axis inflow instability

- Closing the “hole” in the disk makes no (big) difference.
- Numerical issues at $\rho = 0$?

Poloidal cut of $\|\vec{u}\|$

...at $t = 100$, $\Omega = 0$, on a cylindrical grid (where $\rho = 0$ is a grid boundary)

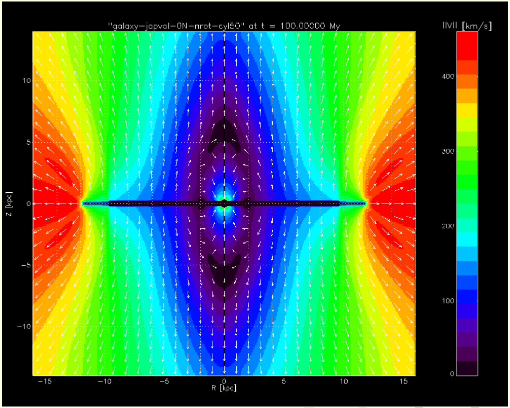

Determining the cause of the near-axis inflow instability

- Closing the “hole” in the disk makes no (big) difference.
- Numerical issues at $\rho = 0$?

Poloidal cut of $\|\vec{u}\|$

...at $t = 100$, $\Omega = 0$, on a Cartesian grid (where $\rho = 0$ is **not** a grid boundary)

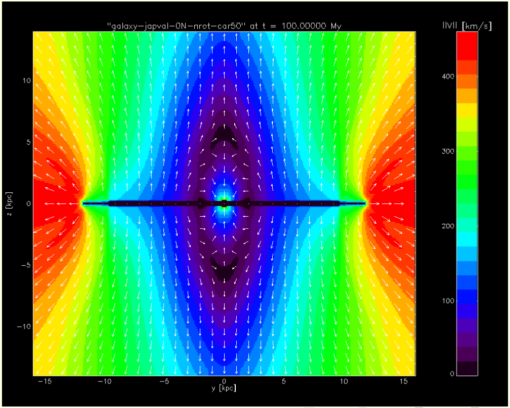

Determining the cause of the near-axis inflow instability

- Closing the “hole” in the disk makes no (big) difference.
- Numerical issues at $\rho = 0$? No, same on Cartesian grid.

Poloidal cut of $\|\vec{u}\|$

...at $t = 100$, $\Omega = 0$, on a Cartesian grid (where $\rho = 0$ is **not** a grid boundary)

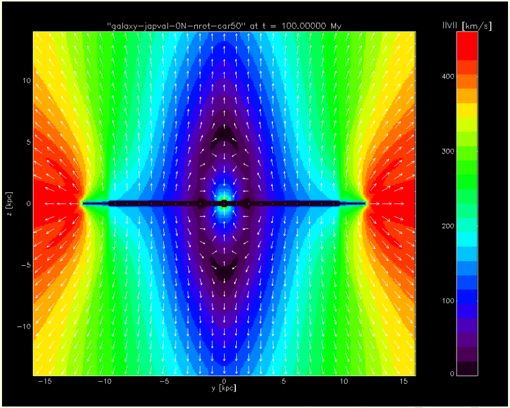

Determining the cause of the near-axis inflow instability

- Closing the “hole” in the disk makes no (big) difference.
- Numerical issues at $\rho = 0$? No, same on Cartesian grid.
- Rotation? Still unstable, but it does widen the inflow region.

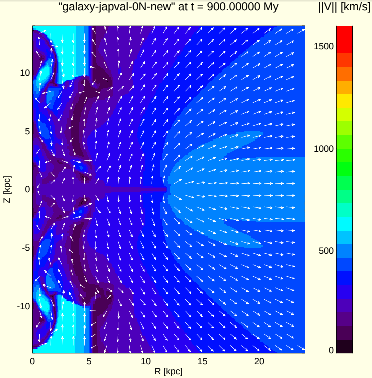

$$\Omega(\vec{r}) = \Omega_{\mathrm{Kepl}}(\vec{r})$$

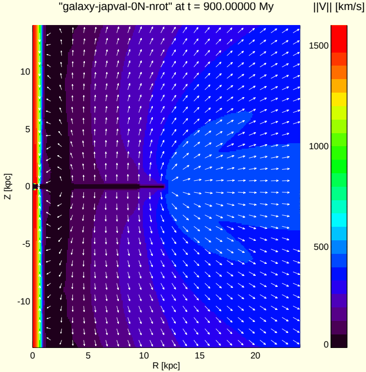

$$\Omega(\vec{r}) = 0$$

Preliminary conclusion

- Crucial distinction: only massive galaxies exhibit the instability. (Trial run for M82 reaches steady-state.)
- Miamoto-Nagai potential has $M_1 + M_2 \approx 27 \cdot 10^{10}\, M_\odot$ (likely based on the Milky Way).
- Starburst galaxies of interest typically are less massive, e.g. $M = (0.9 \ldots 8.6) \cdot 10^{10}\, M_\odot$ [Stein+2023]

Preliminary conclusion

- Crucial distinction: only massive galaxies exhibit the instability. (Trial run for M82 reaches steady-state.)
- Miamoto-Nagai potential has $M_1 + M_2 \approx 27 \cdot 10^{10}\, M_\odot$ (likely based on the Milky Way).
- Starburst galaxies of interest typically are less massive, e.g. $M = (0.9 \ldots 8.6) \cdot 10^{10}\, M_\odot$ [Stein+2023]
- Stationarity seen by Habe & Ikeuchi [1980] might be an artifact of low grid resolution ($N_\rho \times N_z = 22 \times 30$).

Turbulence quantities in the solar wind ($\varphi =$ const. cuts)

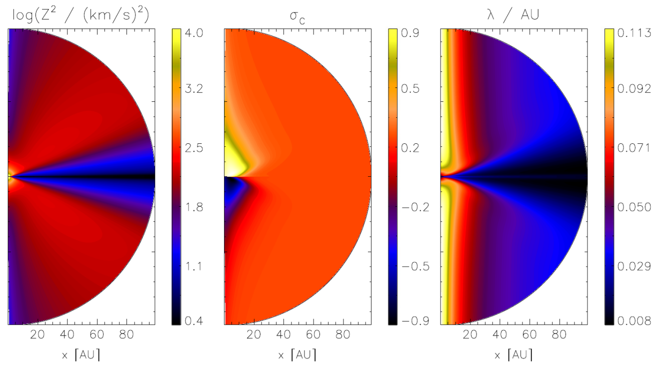

[Wiengarten+2015]

- Z^2 first decreasing with r, then constant
- $|\sigma_\mathrm{c}|$ decreasing (note polarity change with hemisphere)
- λ approx. constant along polar axis

Turbulence seen in (first) galactic wind simulations

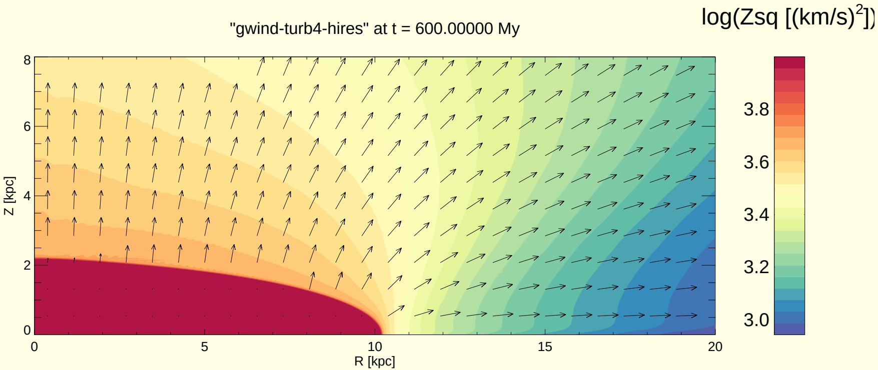

- Z^2 decreasing with r (but smaller dynamic range)

Turbulence seen in (first) galactic wind simulations

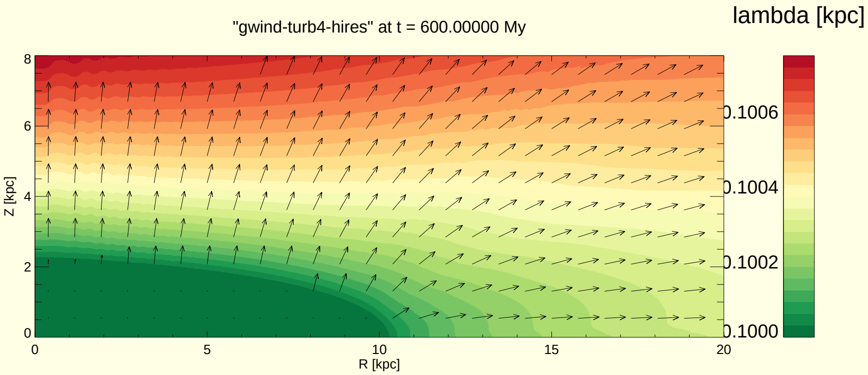

- Z^2 decreasing with r (but smaller dynamic range)
- λ essentially constant

Turbulence seen in (first) galactic wind simulations

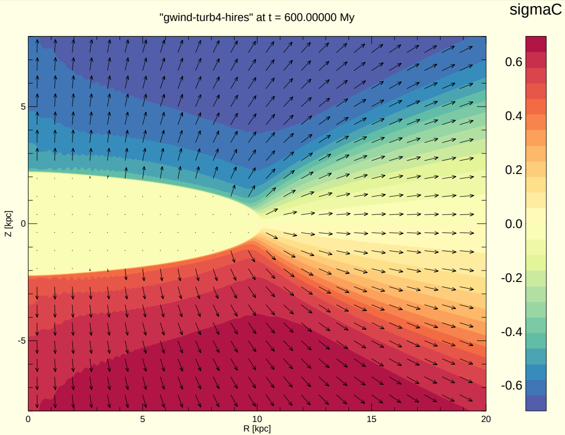

- Z^2 decreasing with r (but smaller dynamic range)
- λ essentially constant
- $|\sigma_{\rm c}|$ increasing from zero(!) (but with polarity change)

Summary and outlook

- A numeric single-fluid (ideal) MHD+turbulence model for a galactic wind is established and tested.
- Origin of axial flow instability traced to galaxy's mass ($\Rightarrow$ likely not relevant for starburst galaxies in **A4**).
- 2D patterns of turbulence in Z^2, σ_c, λ generated (from which $\delta\vec{u}$ and $\delta\vec{b}$ can be found/constrained).

Summary and outlook

- A numeric single-fluid (ideal) MHD+turbulence model for a galactic wind is established and tested.
- Origin of axial flow instability traced to galaxy's mass ($\Rightarrow$ likely not relevant for starburst galaxies in **A4**).
- 2D patterns of turbulence in Z^2, σ_c, λ generated (from which $\delta\vec{u}$ and $\delta\vec{b}$ can be found/constrained).

Imminent next steps:

- Further analysis of differences to heliospheric case
- Then, ready to use "realistic" (= observationally inspired) parameters.

BACKUP SLIDES

1

Hyperbolic fieldlines

...at $t = 0$ allow for a smooth transition of geometry parameters from purely radial ($\propto \vec{e}_r$) to purely vertical ($\propto \vec{e}_z$).

- $\vec{B}$ always $\perp$ to ellipsoidal surface
- Field strength tunable on a per-fieldline basis.

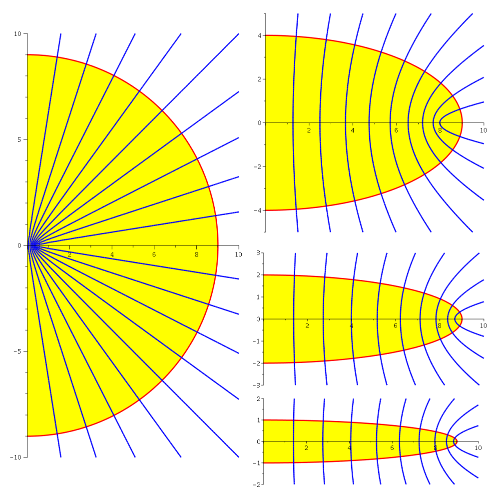

MHD equations with turbulence

$$\partial_t \rho + \nabla \cdot (\rho \vec{U}) = 0$$

$$\partial_t (\rho \vec{U}) + \nabla \cdot \left[\rho \vec{U}\vec{U} + \left(p + \frac{|\vec{B}|^2}{2} + p_{\mathrm{w}} \right) \mathbb{1} - \left(1 + \frac{\sigma_D \rho Z^2}{2B^2} \right) \vec{B}\vec{B} \right] = -\rho \vec{g}$$

$$\partial_t e + \nabla \cdot \left[e\vec{U} + \left(p + \frac{|\vec{B}|^2}{2} \right) \vec{U} - (\vec{U} \cdot \vec{B})\vec{B} \right] + q_{\mathrm{H}} - \frac{\rho H_{\mathrm{c}}}{2} \vec{V}_{\mathrm{A}} + \rho \vec{U} \cdot \vec{g} + \vec{U} \cdot \nabla p_{\mathrm{w}}$$

$$= -(\vec{V}_{\mathrm{A}} \cdot \nabla \rho) \frac{H_{\mathrm{c}}}{2} + \frac{\rho Z^3 f}{2\lambda} + \vec{U} \cdot (\vec{B} \cdot \nabla) \left[\frac{\sigma_D \rho Z^2}{2B^2} \vec{B} \right] - \rho \vec{V}_{\mathrm{A}} \cdot \nabla H_{\mathrm{c}}$$

$$\partial_t \vec{B} + \nabla \cdot (\vec{U}\vec{B} - \vec{B}\vec{U}) = \vec{0}$$

with $H_{\mathrm{c}} \equiv \sigma_{\mathrm{c}} Z^2$, $p_{\mathrm{w}} = (\sigma_D + 1)\rho Z^2/4$, and $\sigma_D = \left\langle \delta u^2 - \delta b^2/n \right\rangle / Z^2 = -1/3$.

The 3-eqn system, to be solved alongside the usual equations of ideal MHD (adapted from a talk by HF)

$$\partial_t Z^2 + \nabla\cdot(\mathbf{U}Z^2 + \mathbf{V}_A Z^2\sigma_C) = \frac{Z^2(1-\sigma_D)}{2}\nabla\cdot\mathbf{U} + 2\mathbf{V}_A\cdot\nabla(Z^2\sigma_C) + Z^2\sigma_D\hat{\mathbf{B}}\cdot(\hat{\mathbf{B}}\cdot\nabla)\mathbf{U} - \frac{\alpha Z^3 f^+}{\lambda} + \langle\mathbf{z}^+\cdot\mathbf{S}^+\rangle + \langle\mathbf{z}^-\cdot\mathbf{S}^-\rangle$$

$$\partial_t(Z^2\sigma_C) + \nabla\cdot(\mathbf{U}Z^2\sigma_C + \mathbf{V}_A Z^2) = \frac{Z^2\sigma_C}{2}\nabla\cdot\mathbf{U} + 2\mathbf{V}_A\cdot\nabla Z^2 + Z^2\sigma_D\nabla\cdot\mathbf{V}_A - \frac{\alpha Z^3 f^-}{\lambda} + \langle\mathbf{z}^+\cdot\mathbf{S}^+\rangle - \langle\mathbf{z}^-\cdot\mathbf{S}^-\rangle$$

$$\partial_t(\rho\lambda) + \nabla\cdot(\mathbf{U}\rho\lambda) = \rho\beta\left[Zf^+ - \frac{\lambda}{\alpha Z^2}\left(\langle\mathbf{z}^+\cdot\mathbf{S}^+\rangle(1-\sigma_C) + \langle\mathbf{z}^-\cdot\mathbf{S}^-\rangle(1+\sigma_C)\right)\right]$$

with $f^\pm = \sqrt{1-\sigma_c^2}\,\frac{\sqrt{1+\sigma_c}\pm\sqrt{1-\sigma_c}}{2}$, $\langle\vec{z}^\pm\cdot\vec{S}^\pm\rangle = \frac{(\partial_t Z^2)_{\text{pui}}}{2}$,
$\vec{V}_A = \vec{B}/\sqrt{\rho}$, and $\hat{\vec{B}} = \vec{B}/B$